A Novel Modified Grasshopper Algorithm for State Estimation of Power System and Design of Renewable Energy Powered Shunt Active Power Filter

Praveen Kumar Balachandran[1,2,*], Dheeraj Sundaragiri[3], Devavarapu Sreenivasarao[3], Shaik Khasim Saheb[3], Harivardhagini Subhadra[4], E. Madhukar[3] and Koganti Srilakshmi[5]

[1] Department of Electrical and Electronics Engineering, Vardhaman College of Engineering, Hyderabad, India

[2] Department of Electrical and Electronics Engineering, Chennai Institute of Technology, Chennai, Tamilnadu, India

[3] Department of Computer Science and Engineering, Sreenidhi Institute of Science and Technology, Hyderabad, India

[4] Department of Electronics and Instrumentation Engineering, CVR College of Engineering, Hyderabad, India

[5] Department of Electrical and Electronics Engineering, Sreenidhi Institute of Science and Technology, Hyderabad, India

INFORMATION

Keywords:
Modified
grasshopper optimization
shunt active power filter
state estimation
total harmonic distortion
power quality

DOI: 10.23967/j.rimni.2026.10.76615

SCIPEDIA Revista Internacional de Métodos Numéricos para Cálculo y Diseño en Ingeniería

Revista Internacional Métodos numéricos para cálculo y diseño en ingeniería RIMNI in cooperation with CIMNE

A Novel Modified Grasshopper Algorithm for State Estimation of Power System and Design of Renewable Energy Powered Shunt Active Power Filter

Praveen Kumar Balachandran[1,2,*], Dheeraj Sundaragiri[3], Devavarapu Sreenivasarao[3], Shaik Khasim Saheb[3], Harivardhagini Subhadra[4], E. Madhukar[3] and Koganti Srilakshmi[5]

[1]Department of Electrical and Electronics Engineering, Vardhaman College of Engineering, Hyderabad, India

[2]Department of Electrical and Electronics Engineering, Chennai Institute of Technology, Chennai, Tamilnadu, India

[3]Department of Computer Science and Engineering, Sreenidhi Institute of Science and Technology, Hyderabad, India

[4]Department of Electronics and Instrumentation Engineering, CVR College of Engineering, Hyderabad, India

[5]Department of Electrical and Electronics Engineering, Sreenidhi Institute of Science and Technology, Hyderabad, India

ABSTRACT

In recent times, meta-heuristic optimization techniques have become indispensable for effectively solving complex engineering problems involving multiple objectives. The Grasshopper Optimization Algorithm (GOA) is a population-based approach inspired by the foraging behaviour of grasshopper swarms. However, the standard GOA may fail to escape sub-optimal solutions, as it does not account for the predator-prey strategy. To address this limitation, this study introduces a modified version of GOA, termed MGOA, which incorporates the predator-prey concept to enhance its ability to avoid local optima and achieve globally optimal solutions. The proposed MGOA is tested on two distinct electric power system challenges. The first optimization problem focuses on the optimal design of a solar system (SS) combined with an energy storage system (ESS) connected to DC bus of the shunt active power filter (SHAPF) to supply an EV charging station and harmonic loads to select filter and gain values of PID controller to minimize THD and maintain stable DC bus voltage (DCBV) to enhance the power quality (PQ) of local distribution network. In addition, to show the superiority of the MGOA, two different test cases were selected with varying loads and partial shading conditions in the solar system. The second optimization problem involves power system state estimation (SE). The goal of SE is realized by employing weighted least square (WELS) or weighted least absolute value (WELAV) criterions where the objective function is formed by minimizing the sum of squares of weighted deviations (SSWD), sum of absolute values of weighted deviations (SAVWD) of estimated measurements from actual measurements Finally, the results highlight the superior performance of MGOA when compared to traditional optimization methods such as Particle Swarm Optimization (PSO) and Genetic Algorithm (GA). However, the proposed method reduces THD to 2.19% with 98% of successes rate with a lower DCBV settling time of 0.03 s while GOA, GA and PSO give that with 3.18%, 3.45%, 3.27% THD with 91%, 88% and 91% of successes rate with higher settling.

OPEN ACCESS

Received: 23/11/2025

Accepted: 03/02/2026

Published: 29/05/2026

DOI
10.23967/j.rimni.2026.10.76615

Keywords:
Modified
grasshopper optimization
shunt active power filter
state estimation
total harmonic distortion
power quality

*Correspondence: Praveen Kumar Balachandran (praveenbala038@gmail.com).

Nomenclature

GOA	Grasshopper Optimization Algorithm
MGOA	Modified Grasshopper Optimization Algorithm
SS	Solar System
ESS	Energy Storage System
SHAPF	Shunt active power filter
EV	Electric Vehicle
DCBV	DC Bus Voltage
THD	Total Harmonic Distortion
SE	State Estimation
PSO	Particle Swarm Optimization
GA	Genetic Algorithm
TS	Tabu Search
ILS	Iterated Local Search
PQ	Power Quality
PF	Power Factor
PIDC	PropotionalIntegral Derivative Controller
SAVWD	Sum of Absolute Values of Weighted Deviations
EM	Estimated Measurements
TM	True Measurements
SSWD	Sum of Squares of Weighted Deviations
WELAV	Weighted Least Absolute Value
WELS	Weighted Least Square
SCV	State Correction Vector
VTM	Voltage Magnitudes
VTA	Voltage Angle
BM	Bad Measurements
PI	Performance Indices
E	Maximum Allowable Error Vector
W	Diagonal Matrix
e	Error Components Vector
Z	Data Set
$R\&L$	Resistance and Inductance
L_{PV}, L_{EES}	Inductance values of solar and battery DC-DC converters
T	Maximum number of iterations
n	Number of design variables
t	Current iteration
c	Decreasing coefficient
$c_{\max}$, $c_{\min}$	Maximum and Minimum values of C
B_k	Best solution in K^{th} dimension till current iteration
μ	Drift's constant
y	GH as control parameter
$\bar{e}_w$	Unity wind vector
g	Gravity constant

$\bar{e}_g$	Earth unity vector
γ_{ij}	Distance between j^{th} and i^{th} GH
$\bar{\gamma}_{ij}$	Unity vector
S	Social force
f	Intensity of attraction
l	Length of attraction
n	No of design variables
FF	Fitness function
Obj	Objective function
S_i	Social force of i^{th} GH
A_i	Wind advection of i^{th} GH
ρ	Hunting rate
η	Hunting propability
ε	Predefined Tolerance
d	Euclidean distance between predator and prey
G_i	Gravitational force of i^{th} GH
r_1, r_2, r_3	Random numbers 0–1
$y_{predator}$	Predator at iteration-t
y_{worst}	Worst solution at iteration-t
V_{DC}	DC Bus Voltage
I_{sh}	Filter compensated current
I_L	Load current
I_s	Source current

1 Introduction

These days, optimization techniques are required to handle a large number of optimization problems in research, engineering, industry, and technology. The three primary components of representing an optimization issue from a mathematical perspective are choice variables, constraints, and objective functions. The goal of optimization is to quantify the problem's choice variables to achieve the objective function1's least (in minimization problems) or maximum (in maximization problems) value while adhering to the restrictions. Techniques used to solve optimization issues can be classified as either stochastic or deterministic. A user requires comprehensive information on comparing problem-solving strategies in order to select the best method for resolving an optimization challenge.

1.1 Literature Survey

For conventional optimization algorithms to handle engineering optimization problems, the problem must be reframed with a specific set of goals and constraints, which is often difficult. They are also struggling with convergent and non-differentiable goal and constraint functions, as well as discontinuous ones. Metaheuristic algorithms, on the other hand, have been employed extensively recently to address a variety real world problems by overcoming the demerits of conventional methods. The evaluation of the objective function is all that is needed for these techniques to search the search space and find the best global solution, in contrast to traditional algorithms that need derivative information.

Because of their well-known severe inefficiency when doing large computations, they are not suitable for real-time applications. However, the advent of parallel processing and the ever-increasing speed of computers have made it possible to overcome the inefficiencies of these algorithms in recent years. Finding the best solution worldwide with the least amount of computational effort is the primary objective of every optimization technique, even for more complex, nonlinear, and bigger problems [1,2].

The two familiar single solution type methods are like simulated annealing [3] and hill climbing [4]. The stochastic cooling effect causes SA to avoid local optima more often, even though the two approaches' ideas are the same. Two additional contemporary methods are TS [5] and ILS [6]. Further, the familiar multi-objective based evolutionary and swarm techniques are GA [7], PSO [8], Ant Colony Optimization [9], and Differential Evolution [10].

The GA algorithm was inspired by the Darwinian theory of evolution. In this approach, the genes of the solutions—which are considered persons—are replaced by the parameters of the solutions. The survival of the fittest theory, which holds that the best individuals are more likely to help improve poor solutions, serves as the main driving force behind this algorithm. The PSO algorithm simulates the foraging behaviour of herds of birds or schools of fish. In this process, the best solutions found by the swarm and the best solutions found by each particle thus far are taken into account while refining the solutions.

By mimicking the collective behaviour of ants, the ACO algorithm determines the fastest path from the nest to the food source. Finally, by combining the parameters of existing solutions using simple formulas, DE enhances the population of possible solutions for a given problem.

Examples of human-based algorithms that imitate everyday human behaviour include Socio Evolution and Learning Optimization [11] and Teaching Learning Based Optimization [12]. The way butterflies forage, using their sense of smell to find nectar or a possible partner, is based on their natural behaviour, which resembles their mating and food hunt [13]. Additionally, the optimization of the hunting behaviour and survival of Flying squirrels and Harris hawks was covered in detail in [14,15].

They are insects, grasshoppers. The distinctive feature of the grasshopper swarm is that it exhibits swarming behaviour throughout its nymphal and adult stages. The grasshoppers' slow motion and tiny steps are the primary traits of the swarm during its larval stage. On the other hand, the key characteristic of the adult swarm is its sudden and long-range movement. Whereas the search agents prefer to travel locally during exploitation, they are urged to move abruptly during exploration. Grasshoppers naturally carry out these two tasks in addition to target finding [16]. The convergence of decoupled versions can become oscillatory and fail to perform estimates, depending on the branch ratio's resistance and reactance as well as the system's loading levels [17]. Both the SE and PQ problems are addressed by football game optimization [18].

Besides, using power electronics devices and non-linear loads leads to the generation of PQ issues like harmonics. A big task of research has led to the creation, marketing, and proposal of numerous strategies to reduce THD. The UPQC is one of the most advanced custom power devices currently being used to increase the PQ of the distribution network. UPQC compensates for PQ disturbances linked to both voltage and current. Voltage distortions and fluctuations are frequent occurrences in weak grid network systems. In order to properly handle PQ difficulties linked to voltage and current, the most valuable player algorithm was used to create the UPQC [19]. To solve the PQ issues brought on by the unbalanced and nonlinear loads, Jaya optimization was used in the design of the shunt power filter [20].

A novel predator-prey firefly optimization algorithm was proposed for SHAPF to reduce Total Harmonic Distortion (THD) [21]. A 15-level reduced-switch multilevel inverter was also introduced for SHAPF, aiming to enhance power quality by providing suitable compensating filter current and minimizing THD [22]. Additionally, a Sliding Mode Control (SMC) with phase-decoupled Kalman filtering was developed to minimize THD, correct power factor, and regulate DC-link voltage under various load and grid conditions in Fuel Cell Electric Vehicle (FCEV) integrated systems [23]. A new optimized proportional-resonant controller was developed by GA for SHAPF for appropriate handling of harmonic currents [24]. Besides, a new adaptive autarchoglossans lizard foraging algorithm was adopted to optimize the instantaneous power control for 3phase SHAPF with a PV array associated to DC-bus with a view to reducing THD [25]. A multi-strategy gradient-based algorithm was developed for the appropriate parameter estimation of solar PV systems [26]. This paper introduces an Improved Moth Flame algorithm with Local escape operators (IMFOL). The LEO technique improves the MFO algorithm's efficiency and the results' precision [27].

1.2 Motivation of Work

These days, optimization techniques are required to handle a large number of optimization problems in research, engineering, industry, and technology. The three primary components of representing an optimization issue from a mathematical perspective are choice variables, constraints, and objective functions. The goal of optimization is to quantify the problem's choice variables in order to achieve the objective function's least (in minimization problems) or maximum (in maximization problems) value while adhering to the restrictions. Techniques used to solve optimization issues can be classified as either stochastic or deterministic. A user requires comprehensive information on comparing problem-solving strategies in order to select the best method for resolving an optimization challenge. On the other hand, more information is frequently required than what the user has access to.

Metaheuristic algorithms have been created and used as competitive alternative solvers for a variety of issues because of their simplicity and convenience of use. Moreover, the basic operations of these methods are independent of the gradient information and mathematical properties of the goal landscape. Nonetheless, a common flaw in the majority of metaheuristic algorithms is that they usually show a low sensitivity to user-specified parameter changes. Another drawback of metaheuristic algorithms is that they cannot always converge to the global optimum.

1.3 Contribution and Novelty

Conventional GOA may struggle to identify the global optimal solution as it overlooks the predator-prey strategy, potentially leading organisms to become trapped in local optima. Similarly, existing literature indicates that metaheuristic algorithms have been evaluated using benchmark test functions. To address this limitation, this research introduces MGOA, an enhanced version of GOA, designed to improve performance and achieve the global optimal solution. MGOA is tested on two distinct real-world complex problems in the power systems domain to demonstrate its numerical stability and robustness. The following points highlight the novelty of this manuscript:

- ✓ Development of a Modified GOA (MGOA) by including the predator-prey concept in the existing GOA and assessing its effectiveness on two real-world electrical engineering challenges.
- ✓ The first problem selected is the PQ problem, which involves the selection of optimal PIDC gain values in addition to R and L filter parameters along with DC-DC converter parameters of PV and battery energy storage L_{PV}, L_{EES} using developed MGOA with an objective of lowering the THD and maintaining stable DLCV.

- ✓ Incorporation of solar PV and battery systems to SHAPF's DC link helps to satisfy load demands by reducing the strain on converters and maintaining a constant voltage in a short amount of time as power management.
- ✓ Performance investigation is carried out with different combinations of loads and partial shading combinations.
- ✓ The second problem is the SEs problem, which examines MGOA on bus systems 6, 14, 30, and 57 using WELS or WELAV criteria to reduce the SAVWD of EM from TM as well as the SSWD.
- ✓ Comparative analysis is carried out with the GOA, GA and PSO to show the ability of the proposed MGOA.

The rest of this article is organised as follows: Section 2 gives a detailed mathematical formulation of the developed MGOA, Section 3 provides a concise overview of the problems selected, i.e., MGOA-based SE and SHAPF, Section 4 provides the outcomes and discussions, and lastly Section 5 concludes the manuscript.

2 Modified GOA Algorithm

2.1 Mathematical Modelling of GOA

The social behaviour of GH during interaction and hunting served as the inspiration for the GOA, a meta-heuristic population-based algorithm. Saremi and Majalili (2017) proposed this algorithm. GOA is most suitable for engineering problems with multi objective. However, the main disadvantage is that GO gets stuck at local optima with premature convergence. Because they lack wings, the swarm travels slowly in tiny movements throuGOAut the nymph phase. During the adult phase, the GH swarm can later use its wings to make abrupt, long-distance leaps. They fly distinctively. Finally, the swarm goes into two phases to find food: exploration and exploitation.

Wind velocity, gravitational force, and interaction are the primary factors governing GH's movement. First, a group of grasshoppers is released into the search area at random. The size of the chosen control variables mostly determines the potential solution for each GH. The solution in GOA is represented by the GH's location within the swarm [16]. The quality of the solution in minimizing the selected objective is represented by GH's fitness function. The GH (y) are randomly generated in the search space. The lower and upper bounds of problem variables are denoted by Eq. (1).

$$\begin{aligned} &y^{dv}\,(\min) \le y^{dv} \le y^{dv}\,(\max) \\ &where, dv = 1....n \end{aligned} \tag{1}$$

Eq. (2) provides i^{th} GH's position.

$$y_i = r_1 S_i + r_2 G_i + r_3 A_i \tag{2}$$

S_i can be calculated by Eq. (3)

$$S_i = \sum_{\substack{j=1 \\ i \neq j}}^{n} s\left(\gamma_{ij}\right) \bar{\gamma}_{ij} \tag{3}$$

$$\gamma_{ij} = \left| y_j - y_i \right| \tag{4}$$

$$\bar{\gamma}_{ij} = \left| y_j - y_i \right| / \gamma_{ij} \tag{5}$$

$$S(r) = fe^{-r/l} - e^{-r} \tag{6}$$

The gravity force of is given by Eq. (7)

$$G_i = -g\bar{e}_g \tag{7}$$

The wind advection of GH can be calculated from Eq. (8)

$$A_i = \mu\bar{e}_w \tag{8}$$

Therefore Eq. (9) can be written as

$$y_i = c\sum_{\substack{j=1 \\ j\neq i}}^{n} s\left(\left|y_j - y_i\right|\right)\frac{y_j - y_i}{\gamma_{ij}} - g\bar{e}_g + \mu\bar{e}_w \tag{9}$$

A few parameters were included to the final mathematical model to improve the exploration and exploitation capacities in order to solve the optimization problems efficiently. Nonetheless, the wind constantly blows in the same direction B_k, and the impact of gravity is essentially insignificant. Consequently, final Eq. (10) is provided below.

$$y^k{}_i = c\left(\sum_{\substack{j=1 \\ j\neq i}}^{n} c\frac{y^k(\max) - y^k(\min)}{2} s\left(\left|y^k{}_j - y^k{}_i\right|\right)\frac{y_j - y_i}{\gamma_{ij}}\right) + B_k \tag{10}$$

The c is updated to enhance exploitation proportional to the number of iteration

$$c = c_{\max} - t\frac{c_{\max} - c_{\min}}{T} \tag{11}$$

2.2 Predator-Prey Concept

When predators follow them, the GHs (prey) find it difficult to remain at their favorite spots and instead search for new, possibly even better, areas that are predator-free. Predators' hunting abilities [21] aid GHs in more efficiently exploring the search area. A tiny hunting probability factor (η) regulates predator hunting, and the predators are modelled using the worst possible outcomes as;

$$y_{predator} = y_{worst}(t) + \rho\left(1 - \frac{t}{T}\right) \tag{12}$$

The GH will try to keep itself far from the predators, which is modelled by the Eq. (12)

$$\begin{aligned} y(t+1) &= y(t) + \rho.e^{-|d|}, \text{if } d > 0 \\ y(t+1) &= y(t) - \rho.e^{-|d|}, \text{if } d < 0 \end{aligned} \tag{13}$$

2.3 Generalised Pseudo-Code of the Developed MGOA with Solution Procedure

The step-by-step process involved in this work for optimization is given below.

1. Starts with the production of random values satisfying constraints
2. Evaluate the fitness function by running the developed model, considering the value of every GH as the required optimal control parameters.
3. Depending on the obtained fitness value, every GH updates its position following the steps in pseudo-code.
4. The iterative process is carried out till it converges.

The parameters selected for the algorithm are listed in Table 1. The pseudo-code of the developed Algorithm 1 is given below:

Table 1: Selected parameters for algorithms

Algorithm	Parameter	Chosen value
GOA	n	10
	l	1.5
	f	0.5
	$C_{\min}$	0.01
	$C_{\max}$	0.9
	T	150
	η	0.02
	ρ	0.045

Algorithm 1: Read the datasuch as load values, resistance and reactance of the line, source voltage details, power system data and measurement values, etc

Select the parameters T, l, n, f, $C_{\min}$, $C_{\max}$ η;
Randomly generate the population of grasshoppers using Eqs. (1), (15) and (25);
Set iteration counter $t = 0$;
Run the simulation and obtain THD Obj using Eq. (16);
Calculate the Obj using Eqs. (28) or (29)
Evaluate the FF of each grasshopper;
Get B_k;
While $(t \leq T)$
Update C *using Eq. (11)*
for each grasshopper do
Normalize the distance between i^{th} *and* j^{th} *grasshopper by Eqs. (2)–(6);*
Update the position of grasshopper by Eq. (10);
Get back the grasshopper if it is out of boundary;
End
Update B *if there is any good solution;*

(Continued)

Algorithm 1 (continued)

If $\left|\dfrac{ybest\,(t) - ybest\,(t-1)}{ybest\,(t-1)}\right| < \varepsilon$
for k consecutive iterations **,** *terminate the loop*
if rand $< \eta$
Hunt j-th grasshopper using Eqs. (12) and (13)
$t = t + 1$;
end while
return B as optimal solution;
End

3 Problems Selected for Testing MGOA

3.1 Problem Formulation for SHAPF

The primary function of a shunt filter is to ensure a distortion-free supply current by injecting the necessary current at the PCC. It effectively addresses issues arising from nonlinear loads, such as poor power factor, harmonic distortion, and current imbalance. Fig. 1 illustrates the schematic diagram of the SHAPF, with the solar and battery designs referenced from [19]. However, many conventional SHAPF design methodologies fail to determine globally optimal parameters. Additionally, the SHAPF's performance can be adversely affected by parameter variations, transient disturbances on the load side, nonlinear behaviour, and other influencing factors.

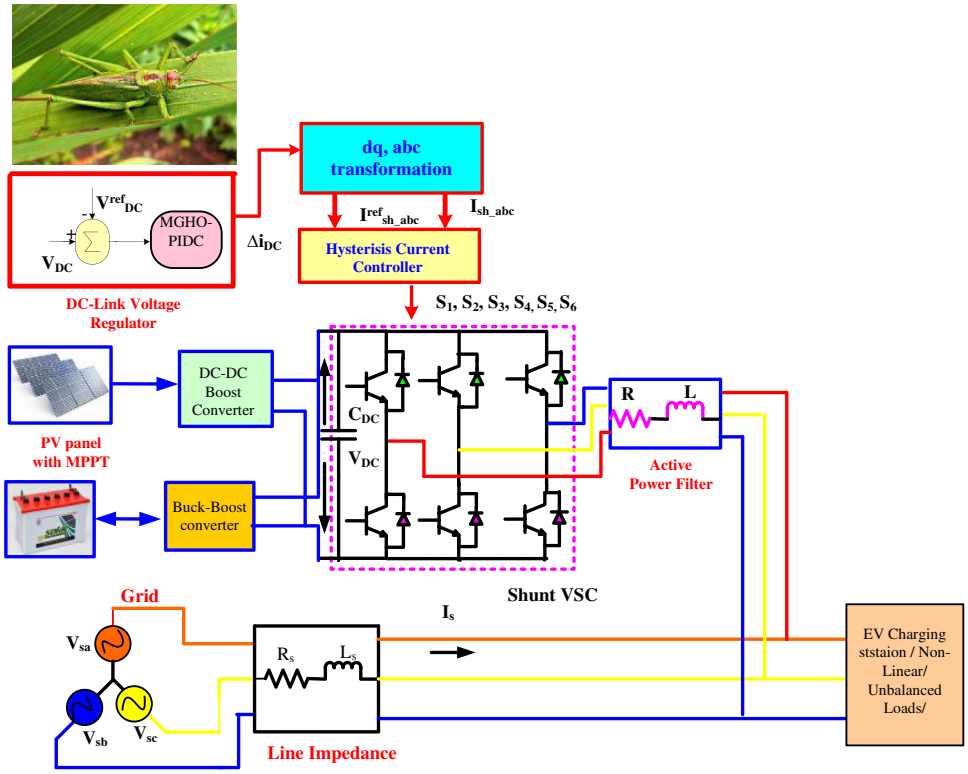

Figure 1: Schematic of renewable powered MGOA designed shunt power filter

The transfer function for the proposed PIDC is given by Eq. (14).

$$TF = K_p + \frac{K_i}{S} + K_d S \tag{14}$$

The proportional, integral, and derivative gains of the suggested PIDC are denoted by K_p, K_i, and K_d in this case. However, PIDC helps to lower the steady state error, which makes the system more stable than other approaches. The design of SHAPF is treated as optimization problem to select filter and gain values of the controller to minimize THD. The MGOA design SHAPF needs the definition of the problem variables. In this case, each GH stands for the design parameters of the SHAPF, with an objective (*obj*) of minimizing THD given by Eqs. (15) and (16)

$$y_i = \left[K_p,\ K_i,\ K_d,\ R,\ L, L_{PV}, L_{ESS}\right] \tag{15}$$

$$Obj = MinTHD \tag{16}$$

Each GH's performance is assessed by calculating the THD using the recommended approach, running the simulation with an EV charging station and a nonlinear rectifier load, and using their fitness as the SHAPF design parameters. The performance of a first group of randomly chosen GH is ascertained by SHAPF simulations. After comparing each GH's performance values with their unique constraints, all of them are either transferred or replaced with those in the nearest, best positions. Following a set number of iterations, the optimal GH location at the point of convergence is identified as the global best value for the SHAPF.

3.2 Problem Formulation for SE

The primary objective of SE is to estimate the system's state by processing the data set z, the error components vector e. The set of nonlinear equations $g(x)$ that follow relates the measurements to the true state vector:

$$z = g(x) + e \tag{17}$$

The SE goal can be accomplished by applying WELS or WELAV criteria [18]. Both solution approaches need the construction of a Jacobian matrix including derivative information. The following subsections provide descriptions of the WELS and WELAV criteria.

3.2.1 WELS Criterion

In this criterion, the prime objective (J) is formed by reducing the SSWD of EM from TM as

$$\text{Min}\, J = [z - g(x)]^T W [z - g(x)] \tag{18}$$

where W indicates a diagonal matrix with measured weights in this case. After partially differentiating J wr.t x, and equating to zero

$$\frac{\partial J}{\partial x} = G^T W \Delta z = 0 \tag{19}$$

here, $G = \dfrac{\partial g(x)}{\partial x}$ and $\Delta z = z - g(x)$.

Eliminating the terms of the higher-order derivative and applying the Taylor series expansion of Eq. (19) yields

$$\left(G^T W G\right) \Delta x = G^T W \Delta z \tag{20}$$

here, when the state correction vector Δx is determined using the solution to Eq. (20), the iteration process x is updated via $(x = x + \Delta x)$ until Δx is smaller than the lower tolerance value. The inverse of the gain matrix $\left(G^T W G\right)$, which necessitates extensive computations and allocates weights of greater values for precise measurements and relatively tiny values for imprecise readings, may leads to problem of convergence. Furthermore, because the objective j also seeks to reduce the bad measurement deviation square from its expected value, processes for detecting and recognizing poor data may be necessary. This means that if some good measures turn bad, the methodology might not yield a trustworthy estimate. Due to these problems, the WELS algorithm is not thought to be strong and dependable.

3.2.2 WELAV Criterion

In this criterion, reducing the SAVWD between the EM and TM is formed as the objective as follows:

$$\text{Min } J = [diag\,(W)]^T\,|z - g\,(x)| \tag{21}$$

Eqs. (15) and (19) can be coupled to create a customized LP problem as

$$\text{Minimize } J = [diag\,(W)]^T\,[e' + e''] \tag{22}$$

Subjected to,

$$G\,\Delta x + e' - e'' = \Delta z \tag{23}$$

$$e',\, e'' \geq 0 \tag{24}$$

here, e' and e'' are slack variables and e by $(e = e' - e'')$

The LP approach can be used to address the aforementioned problem. After selecting a set of good measures from the available data, whose size is equal to the number of state variables, the LP delivers the estimate that exactly fits the chosen measures. At the beginning of the iterative process, the LP attempts to account for any positive measurements that abruptly go wrong and automatically discards them in subsequent iterations. Furthermore, the method is thought to be stable and durable because of its capacity to assign a broad range of weight values for measurements; nonetheless, the LP process is computationally intensive and therefore unsuitable for practical applications.

3.2.3 SE Variables Chosen for MGOA

The SE represents GH in terms of issue variables and develops a cost function or *Obj* using MGOA. In this approach, the SCV is selected as a problem variable. Consequently, it is thought that each GH's position symbolises the SE problem's SCV as

$$\begin{aligned} y_i &= [y_{i,1},\, y_{i,2},\, \cdots, \cdots, \cdots, \cdots, \cdots, \cdots, \cdots\, , y_{i,ns}] \\ &= [\Delta\delta_2,\, \Delta\delta_3,\, \cdots,\, \Delta\delta_{nb},\, \Delta V_1,\, \Delta V_2,\, \cdots,\, \Delta V_{nb}] \end{aligned} \tag{25}$$

The following are the lower and higher boundaries that limit the GH positions:

$$-\Delta\delta^{limit} \leq \Delta\delta \leq \Delta\delta^{limit} \tag{26}$$

$$-\Delta V^{limit} \leq \Delta V \leq \Delta V^{limit} \tag{27}$$

The magnitudes and angles of the correction vectors are very small and can take either positive or negative values. As the correction vectors are treated as unknown decision variables in the problem formulation, their lower and upper bounds are determined heuristically through a trial-and-error procedure. Here, the SCV is utilized as the problem variable, the cost functions from Eqs. (3) and (6) can be written in terms of the GH's position:

$$\text{Min } J = [z - g(x_o + \Delta x)]^T w [z - g(x_o + \Delta x)] \tag{28}$$

$$\text{Min } J = [diag(w)]^T |z - g(x_o + \Delta x)| \tag{29}$$

This is the previously estimated system state vector x_o. Depending on whether the WELS or WELAV criterion is chosen, the GH current fitness level (F) can be used to assess how excellent their circumstances are. The cost function in this problem is the OBF of Eqs. (28) or (29). The F of each GH is calculated.

3.2.4 Recognition and Finding of Bad Measurements (BM)

Bad measurements can be found and detected using the following procedure.

1. The maximum objective value for each measuring unit's predefined maximum permissible error can be found by

$$J^{\max} = [E]^T w [E] \text{ for WELS OBJ} \tag{30}$$

$$J^{\max} = [diag(w)]^T |E| \text{ for WELAV OBJ} \tag{31}$$

here, $J^{\max}$ required to be calculated just once using a data of measurements. By replacing the predicted system state in Eqs. (17)–(21) and comparing with $J^{\max}$ the objective function value (J), one can first identify the existence of BM. If $J < J^{\max}$, then no bad measurements are present and the estimated state of the system is regarded as the real state; else, then single or multiple bad measurements are found.

2. The WEC of $\left\{ w_i [z_i - g_i(x_o + \Delta x)]^2 \right\}$ or $\{ w_i |z_i - g_i(x_o + \Delta x)| \}$ for every measurement has be evaluated once the BM is identified. The highest measurement of WEC is decided as the BM. The detected inaccurate measure is eliminated and $J^{\max}$ recalculated appropriately. The SE is run again and again till $J < J^{\max}$ it is completed.

4 Results and Discussion

4.1 SE

The MGOA performance is investigated on IEEE 6, 14, 30, and 57-bus using data from [18]. The one-line diagram with load statistics for the 6-bus system is shown in Fig. 2. At the conclusion of power flow analysis, real and reactive line flows, real and reactive bus powers, and voltage magnitudes (VTM) are computed. Low noise is then added to these computed values to obtain measurement values. Some of them are chosen in this way to guarantee that the system can be observed and utilized as a set of measurements. Table 2 lists the types of measurements, locations of meters, and p.u value of measurements for the 6-bus system. However, using this measurement set, the MGOA is then performed, accounting for each WELS or WELAV objective separately. Voltage magnitue (VTM = 1.0 per unit) and voltage angles (VTA = 0 radians) are believed to represent the system's prior condition. The results are compared to the system's real state for validation. Furthermore, results from the WELS, WLAV, GOA, GA, and PSO approaches also show how effective the established method is. The cost

function, which is supplied by Eq. (18), is used in both GOA, GA and PSO procedures and is compared to methods from the literature.

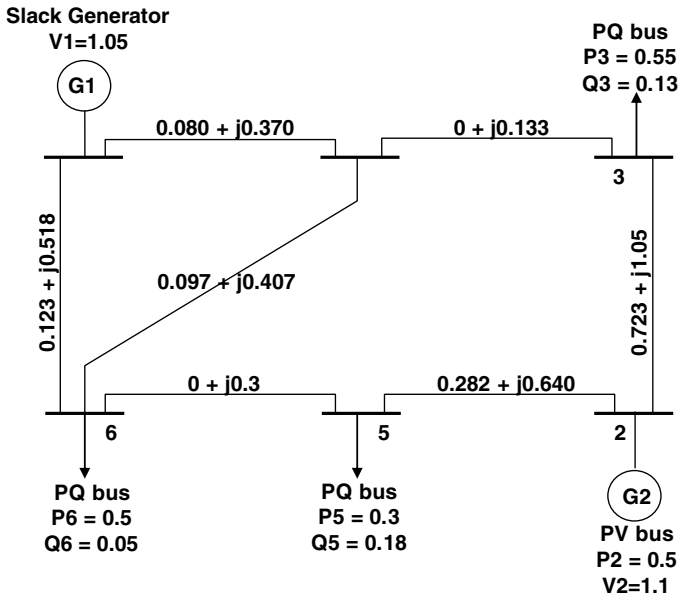

Figure 2: Test 6 bus IEEE system

Table 2: Measurement data for 6-bus system

Measurement	Location/Value in p.u
Reactive power line flow	2/0.138, 4/0.163, 6/−0.055
Reactive bus-power	1/0.314, 2/0.200, 3/−0.129, 4/0, 5/−0.181, 6/−0.049
Real bus-power	1/0.961, 2/0.495, 3/−0.558, 4/0, 5/−0.301, 6/−0.495
Bus voltage magnitude	1/1.073, 3/0.957, 5/0.935
Real power line flow	2/0.437, 4/0.312, 6/0.100

For a 6 bus system without taking bad measurements (BM) into account, Table 3 shows the VTM and VTA of the true and estimated states of the system as determined by all methodologies. The outcomes of the MGOA are very close to those of the conventional WELS and WELAV approaches. The EM and TM differ by a very small value, indicating that the MGOA is accurate enough to achieve SE. However, the results of the GOA, GA and PSO approaches are worse than those of the true system state. Comparison of two sets of numbers may not give quantitative outcomes. To objective evaluate the correctness of the proposed method, the performance indices (PI) for VTM and VTA are evaluated and displayed in Table 4.

$$\Delta V_{rms} = \sqrt{\frac{1}{nb}\sum_{i}^{nb}\left(V_i^t - V_i\right)^2} \tag{32}$$

$$\Delta\delta_{rms} = \sqrt{\frac{1}{nb}\sum_{i}^{nb}\left(\delta_i^{\,t} - \delta_i\right)^2} \tag{33}$$

Table 3: Results comparison for 6-bus network without considering the bad measures

Method		Test bus number					
		1	2	3	4	5	6
MGOA with WELS	VTA	0.000	−0.061	−0.228	−0.170	−0.217	−0.213
	VTM	1.049	1.087	0.941	0.960	0.919	0.943
MGOA with WELS	VTA	0.000	−0.060	−0.234	−0.170	−0.215	−0.212
	VTM	1.047	1.082	0.939	0.959	0.909	0.933
Classical WELS	VTA	0.000	−0.049	−0.305	−0.169	−0.248	−0.216
	VTM	1.060	1.075	0.899	0.973	0.901	0.957
MGOA with WELAV	VTA	0.000	−0.062	−0.229	−0.172	−0.218	−0.214
	VTM	1.050	1.085	0.941	0.959	0.917	0.945
MGOA with WELAV	VTA	0.000	−0.062	−0.229	−0.172	−0.208	−0.204
	VTM	1.049	1.086	0.941	0.957	0.917	0.934
Classical WELAV	VTA	0.000	−0.068	−0.231	−0.169	−0.211	−0.215
	VTM	1.049	1.091	0.942	0.964	0.910	0.936
IFGO [18]	VTA	0.000	−0.062	−0.228	−0.171	−0.218	−0.213
	VTM	1.050	1.086	0.941	0.961	0.918	0.945
GA	VTA	0.000	−0.059	−0.195	−0.147	−0.207	−0.219
	VTM	1.041	1.079	0.897	0.968	0.927	0.951
BF	VTA	0.000	−0.053	−0.225	−0.170	−0.218	−0.209
	VTM	1.040	1.080	0.933	0.953	0.911	0.951
PSO [18]	VTA	0.000	−0.047	−0.210	−0.159	−0.204	−0.203
	VTM	1.076	1.105	0.970	0.989	0.937	0.970
ABC [18]	VTA	0.000	−0.063	−0.234	−0.176	−0.221	−0.218
	VTM	1.052	1.091	0.944	0.963	0.919	0.946
True system	VTA	0.000	−0.063	−0.229	−0.172	−0.219	−0.214
	VTM	1.050	1.086	0.942	0.961	0.918	0.945

Table 4: Performance indices (PI) comparison without BM

Method		Test bus number			
		6	14	30	57
MGOA with WELS	ΔV_{rms}	0.000609	0.000254	0.000218	0.00010
	$\Delta\delta_{rms}$	0.001001	0.000699	0.001507	0.000591
GOA with WELS	ΔV_{rms}	0.000628	0.000354	0.000237	0.00011
	$\Delta\delta_{rms}$	0.001103	0.000703	0.001667	0.000599
Classical WELS	ΔV_{rms}	0.004260	0.000671	0.000538	0.001708
	$\Delta\delta_{rms}$	0.007986	0.001702	0.001498	0.000880
MGOA with WELAV	ΔV_{rms}	0.000679	0.000593	0.000501	0.000103
	$\Delta\delta_{rms}$	0.000301	0.000706	0.001504	0.000701
GOA with WELAV	ΔV_{rms}	0.000679	0.000593	0.000501	0.000103
	$\Delta\delta_{rms}$	0.000331	0.000736	0.001554	0.000711
Classical WELAV	ΔV_{rms}	0.002440	0.002189	0.000671	0.001647
	$\Delta\delta_{rms}$	0.008901	0.000701	0.001114	0.001601
IFGO with WELS [18]	ΔV_{rms}	0.000828	0.000358	0.000258	0.000199
	$\Delta\delta_{rms}$	0.001185	0.000566	0.001475	0.000873
IFGO with WELAV [18]	ΔV_{rms}	0.000669	0.000453	0.000374	0.000103
	$\Delta\delta_{rms}$	0.000339	0.000801	0.001434	0.000726
GA	ΔV_{rms}	0.000918	0.000278	0.000411	0.000200
	$\Delta\delta_{rms}$	0.001255	0.000601	0.001510	0.000912
BF	ΔV_{rms}	0.004350	0.000680	0.000601	0.002108
	$\Delta\delta_{rms}$	0.008176	0.001679	0.001414	0.000989
PSO [18]	ΔV_{rms}	0.013456	0.001212	0.001742	0.009077
	$\Delta\delta_{rms}$	0.024619	0.002781	0.008463	0.008191
ABC [18]	ΔV_{rms}	0.003314	0.000671	0.000490	0.001863
	$\Delta\delta_{rms}$	0.002657	0.001603	0.001282	0.000967

The PI that calculated for all the techniques is listed in Table 3, which does not include the data for 14, 30, or 57 bus systems. However, it is clearly visible that the r.m.s. error component of the MGOA is lower than that of the available techniques for all test systems. The GOA, PSO and GA approaches yields unsatisfied results. The ability of the proposed MGOA with BM was examined by randomly selecting three measurements in the 57-bus test system and setting them to zero to make them BM.

Here, the MGOA is applied to the measured set with BM and PI $\Delta\delta_{rms}$ (radian) and ΔV_{rms} (p.u) were evaluated from the estimated state of the system. Figs. 3 and 4 provide the graphical representation of the computed PI, which makes it evident that $\Delta\delta_{rms}$ and ΔV_{rms} of the MGOA with WELS and WELAV objectives is significantly lower than the available approaches. For example, with a set of measurements without BM, the ΔV_{rms} of MGOA with WELS and WELAV is 0.0001 and 0.000103, respectively. The estimate of the MGOA is minimized by the inclusion of BM, ΔV_{rms} to 0.000792 and 0.000416 for WELS and WELAV objectives, respectively. Compared to the WELS, WLAV, GOA, GA, and PSO methods, as well as other approaches found in the literature, the increase in ΔV_{rms} values following the addition of BM is negligible.

This work exhibits that by eliminating the erroneous data, the MGOA technique is a reliable algorithm that can effectively predict the system state.

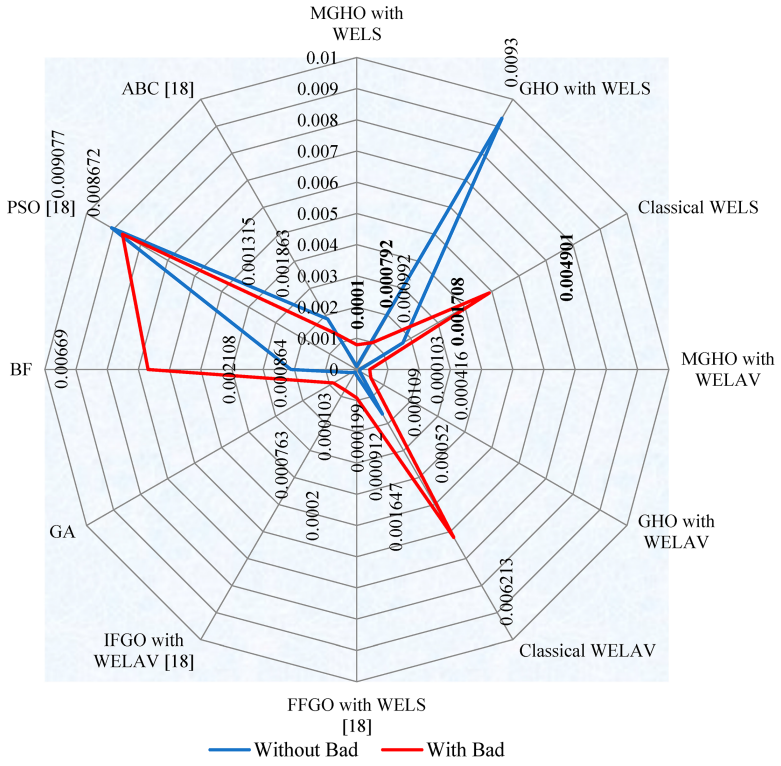

Figure 3: PI of ΔV_{rms} (p.u) of all techniques for the 57-bus system by considering and eliminating BM [18]

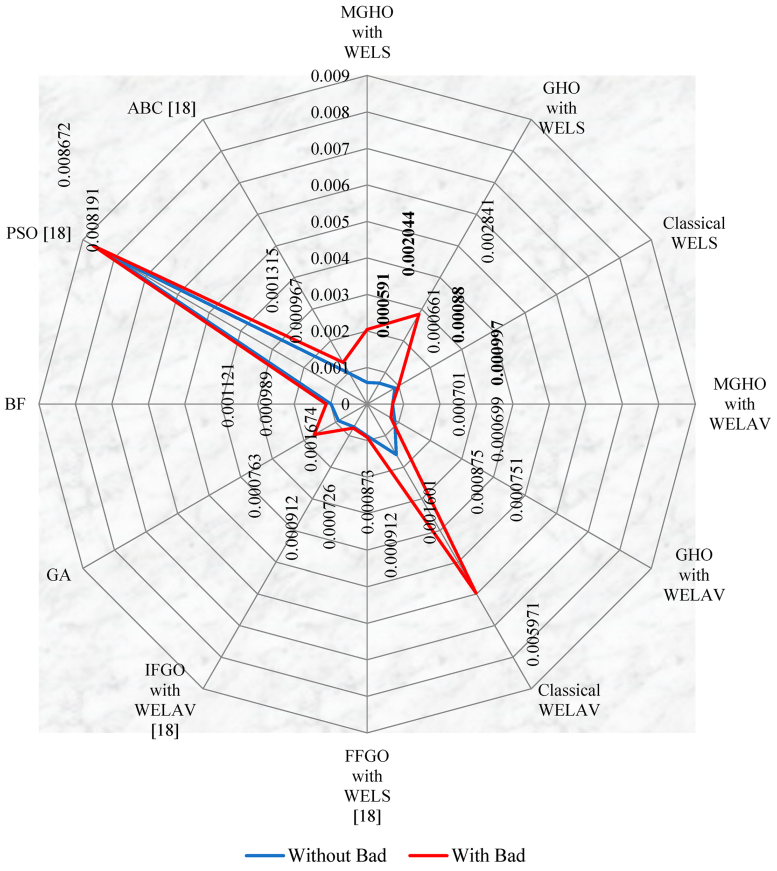

Figure 4: PI of $\Delta\delta_{rms}$ (radian) of all techniques for 57-bus system by considering and eliminating BM [18]

4.2 MGOA for Design of SHAPF

This study examines the performance of MGOA under partial shading with a combination of EV charging station, non-linear rectifier and unbalanced RL loads (the load values taken in this research are listed in the Appendix A). Using the MATLAB environment, the proposed design technique, including MGOA has been investigated in the design of SHAPF parameters and controllers for a 3Φ, 415 V AC system. To demonstrate the superior performance of the suggested MGOA approach, the SHAPF was also built utilizing GA and PSO. The waveforms of the chosen system's V_{DC}, I_{sh}, I_s, and I_L under varied irradiation are shown in Fig. 5.

Here, the I_L (Fig. 5a) is non-sinusoidal and balanced till 0.5 s. However, after at 0.5 s, the unbalanced RL load is connected, due to which unbalances exist in the load current. In the absence of a suitable compensating device, the non-sinusoidal current impairs the performance of the grid and other connected equipment. The MGOA designed SHAPF injects the suitable filter current that makes the source current balanced sinusoidal. However, Fig. 5b exhibits the varying irradiation considered for PV panels, and it is also clearly visible that the proposed method optimally selects the gain values and stabilizes the V_{DC} in a very short time, less than 0.05 s.

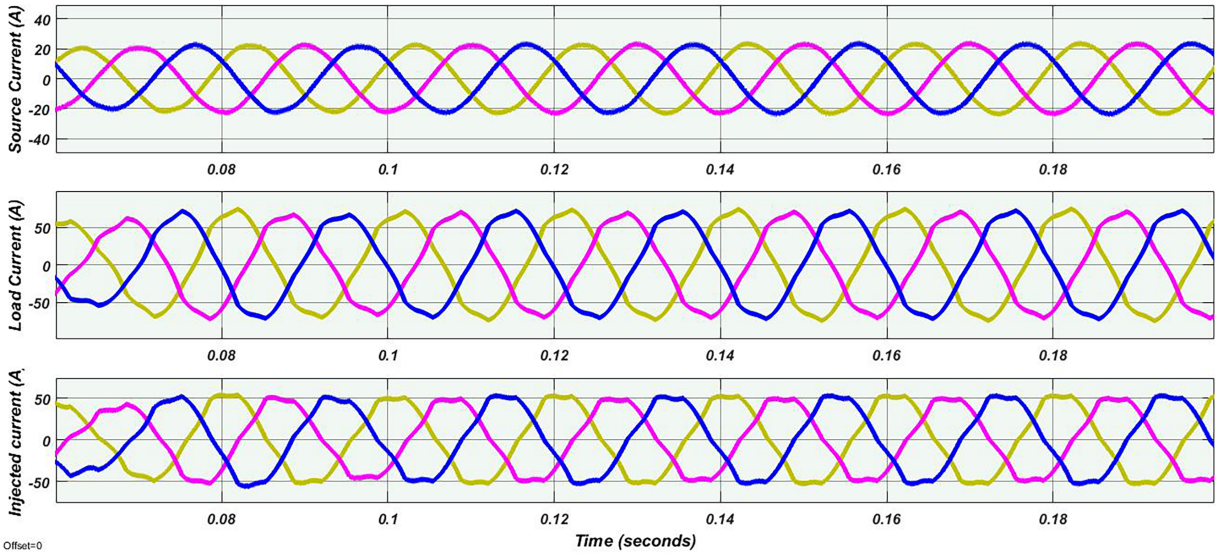

(a) Source, compenstaed, load currents

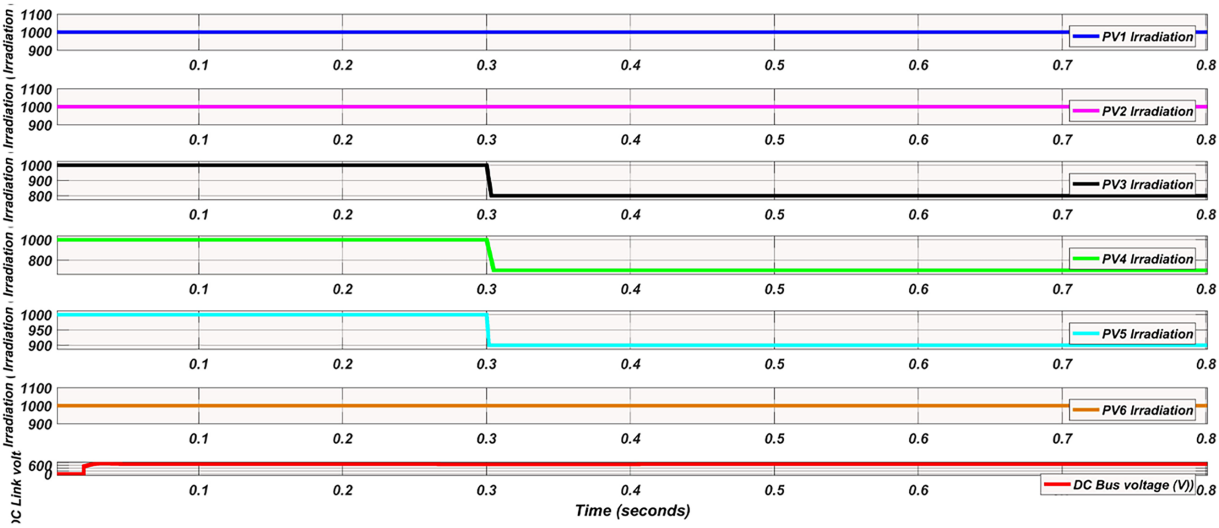

(b) Variable Irradiation of PV pannels, DC link voltage

Figure 5: MGOA designed SHAPF waveforms

Table 5 compares the THD and DC bus voltage settling time (s) and its % of steady state error (%e_{ss}), rise time (t_r), peak overshoot (M_p), and settling time is within ±2% computed at PCC prior to and following the connection of the MGOA-designed SHAPF. Fig. 6 displays the proposed method's FFT spectrum, and Fig. 7 provides the convergence graph, which reveals that MGOA reaches to THD in a lower number of iterations i.e., 26 when compared to GOA, GA, and PSO with 33, 42, 47 iterations. The MGOA (100 runs) can lower the THD from its initial value of 14.015% to 2.19%, which is a substantial decrease from what its rivals can achieve. The supply current is made exactly sinusoidal by the developed method. It is clear from the previous discussions that the developed approach can raise the PQ by bringing the THD down to within the 5% limit of the IEEE 519-2014 standard, which results in a sinusoidal supply current. The %THD of the proposed algorithm have not been presented but

analysed for the design of SHAPF. With a view of studying the robustness of the developed methods, the minimum, maximum and average %THD over 100 runs have been presented in Table 6. It also includes the success rate. It can be revealed from the table that the average cost function value (CFV) of the PDM is very close to the lowest %THD among other methods. Besides, the success rate over 100 trials is greater than that of other strategies. The greater success rate and smaller %THD project the robustness of the developed algorithm.

Table 5: Performances comparison

Method	%THD	V_{DC} Settling time (s)	$\%e_{ss}$	t_r (s)	$\%M_p$
MGOA	2.19	0.03	0.6	0.03	0.6
GOA	3.18	0.05	0.7	0.06	0.9
GA	3.45	0.09	0.8	0.07	1.8
PSO	3.27	0.08	0.8	0.06	1.3

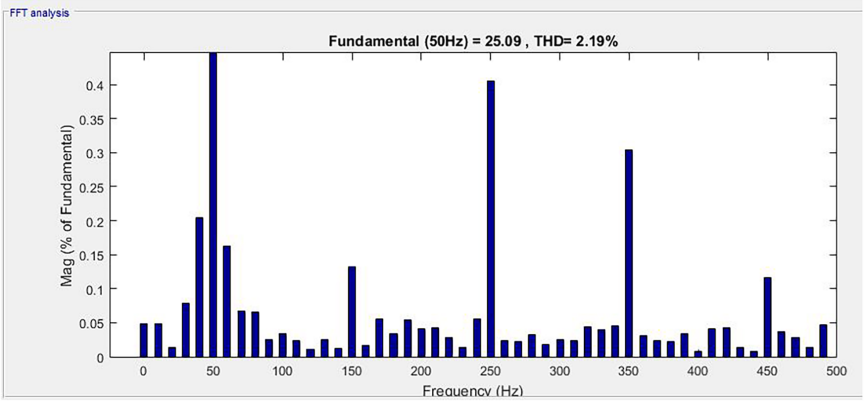

Figure 6: FFT spectrum for current for proposed method

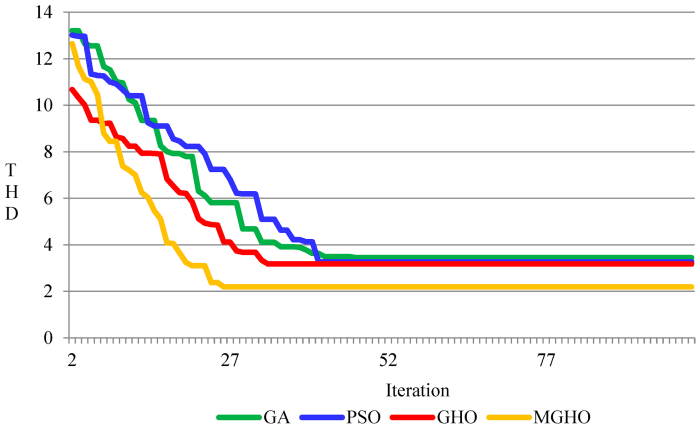

Figure 7: Convergence plot

Table 6: Statistical analysis

Method	(%THD)			Success rate (%)
	Maximum	Minimum	Average	
MGOA	2.23	2.19	2.21	98
GOA	3.21	3.18	3.21	91
GA	3.69	3.45	3.57	88
PSO	3.45	3.27	3.36	91

5 Conclusion

GOA is a population-based method that uses the convergence, stability, and robustness of the algorithm to solve real-world issues by randomly assigning GH. The construction of a modified version of GOA, i.e., MGOA, is to improve its effectiveness by accounting for the predator-prey topic of this study. In this work, the developed algorithm performance was tested on: (1) optimal design of SHAPF's parameters with optimal selection of gain values of PID controller to minimize THD and (2) static SE problem which has been adapted to choose either WELS or WELAV objective without drastically altering the algorithm flow with objective function is formed by minimizing the SSWD, SAVWD of EM from TM. The evaluated PI shows that the system state of the developed technique closely resembles the true system state for each test system. BM effects on the 57 bus system have also been investigated, and it has been shown that the recommended method is capable of rejecting the BM. On the other hand, the proposed method reduces THD to 2.19% with 98% of successes rate, with a lower DCBV settling time of 0.03 s much better when compared to other techniques. Therefore, the developed MGOA is reliable, steady, and effective. By lowering voltage distortions and THD to the lowest possible value, MGOA in SHAPF design illustrates the algorithm's dominance in generating the most effective global design. Future works studies on the convergence of the hybrid algorithm with self-adaptive techniques to modify its parameters and concentrate on a range of optimization issues, such as dynamic state estimation, power management, and unit commitment.

Acknowledgement: Not applicable.

Funding Statement: The authors received no specific funding.

Author Contributions: The authors confirm contribution to the paper as follows: study conception and design: Praveen Kumar Balachandran, Koganti Srilakshmi and Harivardhagini Subhadra; data collection: Dheeraj Sundaragiri, Devavarapu Sreenivasarao, Shaik Khasim Saheb and E. Madhukar; analysis and interpretation of results: Praveen Kumar Balachandran, Koganti Srilakshmi, Harivardhagini Subhadra, Dheeraj Sundaragiri, Devavarapu Sreenivasarao, Shaik Khasim Saheb and E. Madhukar; draft manuscript preparation: Koganti Srilakshmi and Praveen Kumar Balachandran. All authors reviewed and approved the final version of the manuscript.

Availability of Data and Materials: The data that support the findings of this study are available from the Corresponding Author, Praveen Kumar Balachandran, upon reasonable request.

Ethics Approval: Not applicable.

Conflicts of Interest: The authors declare no conflicts of interest.

References

1. Yang XS. Nature-inspired metaheuristic algorithms. 2nd ed. Exeter, UK: Luniver Press; 2016.
2. Davis L. Bit-climbing, representational bias, and test suite design. In: Proceedings of the Fourth International Conference on Genetic Algorithms. New York, NY, USA: Morgan Kaufmann Publishers; 1991. p. 18–23.
3. Kirkpatrick S, Gelatt CD Jr, Vecchi MP. Optimization by simulated annealing. Science. 1983;220(4598):671–80. doi:10.1126/science.220.4598.671.
4. Fogel LJ, Owens AJ, Walsh MJ. Artificial intelligence through simulated evolution. In: Evolutionary computation: the fossil record. Hoboken, NJ, USA: John Wiley & Sons, Inc.; 1966. p. 221–62.
5. Glover F. Tabu search: part I. ORSA J Comput. 1989;1(3):190–206. doi:10.1287/ijoc.1.3.190.
6. Ramalhinho Dias Lourenço H, Martin OC, Stutzle T. Iterated local search. SSRN J. 2001;44:1–42. doi:10.2139/ssrn.273397.
7. Holland JH. Genetic algorithms. Sci Am. 1992;267(1):66–73. doi:10.1038/scientificamerican0792-66.
8. Eberhart R, Kennedy J. A new optimizer using particle swarm theory. In: Proceedings of the the Sixth International Symposium on Micro Machine and Human Science; 1995 Oct 4–6; Nagoya, Japan. p. 39–43. doi:10.1109/MHS.1995.494215.
9. Colorni A, Dorigo M, Maniezzo V. Distributed optimization by ant colonies. In: Proceedings of the First European Conference on Artificial Life; 1991 Dec 11–13; Paris, France. p. 134–42.
10. Storn R, Price K. Differential evolution-a simple and efficient heuristic for global optimization over continuous spaces. J Glob Optim. 1997;11(4):341–59. doi:10.1023/A:1008202821328.
11. Kumar M, Kulkarni AJ, Satapathy SC. Socio evolution & learning optimization algorithm: a socio-inspired optimization methodology. Future Gener Comput Syst. 2018;81:252–72. doi:10.1016/j.future.2017.10.052.
12. Rao RV, Savsani VJ, Vakharia DP. Teaching-learning-based optimization: an optimization method for continuous non-linear large scale problems. Inf Sci. 2012;183(1):1–15. doi:10.1016/j.ins.2011.08.006.
13. Arora S, Singh S. Butterfly optimization algorithm: a novel approach for global optimization. Soft Comput. 2019;23(3):715–34. doi:10.1007/s00500-018-3102-4.
14. Heidari AA, Mirjalili S, Faris H, Aljarah I, Mafarja M, Chen H. Harris Hawks optimization: algorithm and applications. Future Gener Comput Syst. 2019;97:849–72. doi:10.1016/j.future.2019.02.028.
15. Azizyan G, MiarNaeimi F, Rashki M, Shabakhty N. Flying squirrel optimizer (FSO): a novel SI-based optimization algorithm for engineering problems. Iran J Optim. 2019;11(2):177–205.
16. Saremi S, Mirjalili S, Lewis A. Grasshopper optimisation algorithm: theory and application. Adv Eng Softw. 2017;105:30–47. doi:10.1016/j.advengsoft.2017.01.004.
17. Aravindhababu P, Neela R. A reliable and fast-decoupled weighted least square state estimation for power systems. Electr Power Compon Syst. 2008;36(11):1200–7. doi:10.1080/15325000802084687.
18. Subramaniyan S, Ramiah J. Improved football game optimization for state estimation and power quality enhancement. Comput Electr Eng. 2020;81(3):106547. doi:10.1016/j.compeleceng.2019.106547.
19. Srilakshmi K, Gaddameedhi S, Borra SR, Balachandran PK, Reddy GP, Palanivelu A, et al. Optimal design of solar/wind/battery and EV fed UPQC for power quality and power flow management using enhanced most valuable player algorithm. Front Energy Res. 2024;11:1342085. doi:10.3389/fenrg.2023.1342085.
20. Srilakshmi K, Santosh DT, Ramadevi A, Balachandran PK, Reddy GP, Palanivelu A, et al. Development of renewable energy fed three-level hybrid active filter for EV charging station load using Jaya grey wolf optimization. Sci Rep. 2024;14(1):4429. doi:10.1038/s41598-024-54550-7.

21. Mahaboob S, Ajithan SK, Jayaraman S. Optimal design of shunt active power filter for power quality enhancement using predator-prey based firefly optimization. Swarm Evol Comput. 2019;44(5):522–33. doi:10.1016/j.swevo.2018.06.008.
22. Das Biswas S, Das B, Das SS, Nandi C, Shuaibu HA, Ustun TS. Enhanced power quality with 15-level reduced switch count multi-level inverter based shunt active power filter. Results Eng. 2025;27(2):106543. doi:10.1016/j.rineng.2025.106543.
23. Erel MZ. Fuel-cell electric vehicle integrated shunt active power filter with advanced control algorithm for energy management and harmonic suppression. Eng Sci Technol Int J. 2025;72:102241. doi:10.1016/j.jestch.2025.102241.
24. Amini B, Rastegar H, Pichan M. An optimized proportional resonant current controller based genetic algorithm for enhancing shunt active power filter performance. Int J Electr Power Energy Syst. 2024;156(1):109738. doi:10.1016/j.ijepes.2023.109738.
25. Khalid S. A novel algorithm adaptive Autarchoglossans lizard foraging (AALF) in a shunt active power filter connected to MPPT-based photovoltaic array. E Prime Adv Electr Eng Electron Energy. 2023;3:100100. doi:10.1016/j.prime.2022.100100.
26. Mahmood BS, Hussein NK, Aljohani M, Qaraad M. A modified gradient search rule based on the quasi-Newton method and a new local search technique to improve the gradient-based algorithm: solar photovoltaic parameter extraction. Mathematics. 2023;11(19):4200. doi:10.3390/math11194200.
27. Qaraad M, Amjad S, Hussein NK, Badawy M, Mirjalili S, Elhosseini MA. Photovoltaic parameter estimation using improved moth flame algorithms with local escape operators. Comput Electr Eng. 2023;106:108603. doi:10.1016/j.compeleceng.2023.108603.

Appendix A

Appendix A.1 Loads and Specifications of Designed System

Grid voltage = 415 V, frequency = 50 Hz; loads: Rectifier bridge RL 30 Ω, and 60 mH; Un equal phase load: $R_1 = 10$, $R_2 = 100$ & $R_3 = 190$ Ω; $L_1 = 11.55$ mH, $L_2 = 14.50$ mH& $L_3 = 18.50$ mH; $V_{dc} = 700$ V; $C_{dc} = 2200$ μF.

Appendix A.2 Storage Battery and Solar Parameters

PV panel type = SPR-305E-WHT-D; $N_p/N_s = 11/5$; max P_{PV}: 305.226 W; $I_{PV} = 5.58$ A; OCV: 64.2 V; SCC: 5.96 A; Battery type = Nickel metal hydrate; voltage = 500 V; state of charge = 60%; capacity: 100 Ah.